TECHNICAL UNIVERSITY OF CLUJ-NAPOCA

ACTA TECHNICA NAPOCENSIS

Series: Applied Mathematics, Mechanics, and Engineering
Vol. 69, Issue Special III, July, 2026

WIND AND PAYLOAD AWARE FEASIBILITY MODELLING FOR UAV MOUNTAIN RESUPPLY: A REPRODUCIBLE BUCEGI MOUNTAINS CASE STUDY

Gheorghe MINCULETE, Dragoș GHERGHINOIU

Abstract: *We present a reproducible, equation-based framework for UAV resupply in mountainous terrain, where feasibility is driven by coupled headwind time and payload energy effects. A compact multirotor power model, wind-aware segment timing, and an explicit battery-reserve policy form a single feasibility test, visualized as headwind payload envelopes and energy sensitivity curves. The method is demonstrated on a Bucegi Mountains network (Sinaia depot, Piatra Arsă micro-hub, Babele and Omu) and yields payload-tier go/no-go rules, including a sharp wind cliff as headwind approaches the commanded-airspeed limit (tested to 6 m/s).*
Keywords: *UAV logistics, mountain resupply, wind-aware feasibility, energy consumption modelling, payload wind coupling, micro-hub staging*

1. INTRODUCTION

Supplying isolated mountain communities remains a persistent logistics challenge because terrain, seasonality, and infrastructure constraints make routine transport slow and fragile. This is captured in the field observation that Nepal has some of the most rugged and difficult terrain in the world, making delivery of emergency life-saving products to remote areas challenging [1]. Similar terrain-driven constraints are also reported in academic work on Nepal's vaccine distribution. For example, Thapa and Thapa state that "The mountainous terrain of Nepal presents significant logistical hurdles to traditional vaccine distribution methods"[2].

In such settings with limited access, unmanned aircraft systems are increasingly treated as a complementary transport option. From a humanitarian supply-chain perspective, drones enable in-country delivery of health commodities in access-constrained situations and have been used for deliveries to mountainous regions [3]. This broader uptake is also reflected in the health-supply-chain literature: "Drones are increasingly being used globally for the support of healthcare programmes"[4].

Zipline's model is presented as having the potential to strengthen public supply chains and save lives, with operational performance summarized by the claim that facilities can receive products within 45 minutes versus a conventional turnaround that ranges from 8-21 days [5]. In a retrospective, cross-sectional evaluation of Rwanda's drone blood-delivery service, Nisingizwe et al. conclude: "We found that drone delivery led to faster delivery times and less blood component wastage in health facilities"[6].

Another motivation is defence logistics in contested/denied environments, where aerial resupply can reduce exposure and bypass terrain denial. In that context, drones are associated with remote locations where access by conventional means is difficult or impossible [7]. Extending mountain drone logistics at scale requires integrated airspace services, digital coordination,

and risk controls because feasibility is increasingly influenced by regulatory and service frameworks. At the EU level, harmonised connectivity and services are framed as necessary because they should be established to ensure the safe, secure and efficient operation of UAS [8]. Within UTM policy and technical discussions, localized weather becomes an explicit service requirement via forecasting and dissemination of micro-weather to address localized weather patterns [9].

Technically, mountain missions are constrained by limited energy margins, payload coupling, and environmental uncertainty. In addition, UAV capability is constrained because the amount of energy they consume is a determining factor in their ability to achieve their full potential [10]. Planning models that ignore battery and payload couplings risk producing costly or infeasible routes [11], and failing to account [for battery performance] leads to considerable inaccuracy in estimating the amount of available energy [10]. In addition, wind sensitivity amplified by ridge/valley flows creates variance that must be managed, given that the energy cost of a UAV is fiercely affected by the airflow [12].

This article aims to deliver a reproducible, equation-based feasibility screening test for mountainous UAV resupply that couples wind-dependent segment time, payload-dependent power, and an explicit battery-reserve policy. We ask: (RQ1) how do along-track headwind and payload jointly shape the energy-feasibility boundary under a fixed reserve, and (RQ2) how much does plateau micro-hub staging enlarge the feasible payload–headwind region versus direct valley-to-plateau sorties. Overall, we use a quantitative, model-based computational approach (equation-based modelling with specification-based calibration) and a reproducible numerical case-study evaluation, including sensitivity analysis.

2. BACKGROUND AND RELATED WORK

Mountain resupply combines constrained ground access, highly variable local meteorology, and restricted mass and energy budgets for aerial platforms. In the mountain last-mile context, ground transport can become often inefficient, because the customer nodes in mountain cities are scattered and relatively far away [13] and the road network itself is penalized by curvature, gradients, and bottlenecks. These characteristics motivate hybrid logistics approaches (ground + UAV) and, in parallel, fully aerial delivery concepts for destinations that are intermittently or persistently unreachable by conventional vehicles.

From a doctrinal logistics perspective, drones are framed as enabling Just-in-Time replenishment under access and exposure constraints [7]. For mountainous supply in particular, the operational objective is usually not minimum distance but mission feasibility under safety and energy constraints, with repeatable performance envelopes in wind, cold, and reduced density conditions.

2.1 Mountain meteorology as a systems constraint

A key difference of mountainous UAV logistics relative to lowland parcel delivery is the frequency of wind shear, channelling, rotor turbulence, and wave phenomena driven by complex orography. This is reflected in the observation that meteorological and topographical conditions in Norway (and in many other parts of the World) represent severe challenges for UAV operations [14].

Operationally, acceptable wind envelopes limit service reliability, because VTOL platform tolerances can range from 14 m/s to more than 23 m/s [15]. For mountainous resupply, these limits are typically reached more often than in sheltered urban corridors, so realistic logistics concepts require an explicit link between meteorological conditions and routing/energy feasibility rather than treating wind as a secondary consideration.

From a planning perspective, wind is not only a safety hazard but an optimization variable. A route that is geometrically shortest can be energetically inferior when heading into sustained headwinds or when return legs face adverse flow. This supports wind-aware planning, as captured

by findings that energy-aware planning can save at least 30% and 60%, respectively, of the energy consumed in favourable-wind settings [16]. For mountain resupply, the implication is that feasibility and performance claims should be anchored in a wind-aware cost model and visualized with sensitivity plots.

2.2 Energy modelling, payload effects, and demonstrability

A common thread in UAV logistics is that performance cannot be supported convincingly without a transparent energy model that accounts for payload and manoeuvring. Rotorcraft systems are particularly sensitive, since a large proportion of their energy is consumed by rotors [17]. This is particularly relevant for mountainous supply missions where payload fractions can be high and where climb segments (or repeated altitude corrections in turbulence) concentrate energy draw into short windows.

The literature also supports the position that optimization should be posed in physically interpretable terms rather than purely heuristic distance minimization, because an optimal control problem is formulated and solved in order to compute minimum energy [17].

For the present article's practical component, this provides a direct link to practical demonstration:

(i) define a tractable power/energy model;

(ii) integrate wind and altitude effects into effective airspeed and required thrust;

(iii) compute feasible mission sets and compare them graphically across scenarios (payload tiers, wind roses, altitude profiles).

2.3 Routing and scheduling under wind and load coupling

Delivery-drone routing research has progressively moved beyond distance-only objectives, but mountain supply exposes gaps where wind load coupling must be central. Wind and payload-sensitive flight speed is a primary driver of feasibility and service time; therefore, formulations that bind travel time to both load and wind are directly relevant. Ito et al. propose a VRP formulation for drone delivery in which flight time is dependent on the weight of packages in a windy environment, termed the Flight Speed-aware Vehicle Routing Problem with Load and Wind (FSVRPLW) [18].

This is highly relevant to mountainous logistics, where sustained headwinds on exposed ridgelines can coincide with maximum payload segments (outbound legs), i.e., the worst-case combination for energy and time reserves.

Feasibility rather than merely optimality also appears as a central research objective when wind variation is introduced. This is captured by the observation that we study the feasibility of sending drones to deliver goods under wind-driven cost changes [19].

In mountainous resupply, feasibility must be interpreted as a joint condition: energy sufficiency with reserve margins, time constraints (e.g., daylight windows), and safety/regulatory acceptability for the operational volume.

At the scheduling layer, wind uncertainty motivates robust formulations that use observed data rather than fixed safety factors. A representative approach is the use of adaptive robust optimization, where data-driven adaptive distributionally robust optimization (DRO) model leverages wind observations to improve schedules [20]. This has direct operational relevance for mountain corridors where short-term forecasts can be unreliable and where the wind field can shift faster than a sortie cycle.

2.4 Regulatory and navigation-enablement context for European operations

Because mountainous resupply will frequently imply BVLOS segments, sparse population overflight considerations, and constrained emergency landing options, the specific category is often the practical regulatory regime in Europe. In this context, the risk assessment methodology is central, and it is explicitly noted that SORA (Specific Operations Risk Assessment) is included as Acceptable Means of Compliance within EASA Regulation [21].

2.5 Synthesis and identified gap

Across these strands, the literature supports three essential requirements for a mountain UAV-resupply concept:

(i) a physically interpretable, payload-sensitive energy model;

(ii) explicit wind coupling at both feasibility and optimization levels;

(iii) an operational framing that is compatible with structured European risk methodologies.

We close this gap by an integrated, reproducible framework that couples wind, payload, and reserves, and reports results via feasible-region and sensitivity plots.

3. SYSTEM MODEL AND PROBLEM FORMULATION

3.1 Scenario and notation

We consider a depot 0 and a set of mountain demand nodes $V = \{1, \dots, n\}$. Each node i is characterized by geographic coordinates (latitude/longitude), altitude (m), and a required payload (kg). A mission is defined as a route π that starts at the depot, serves one or more nodes, and returns to the depot. For clarity, Eqs. (1) – (2) and (5) – (7) are standard definitions included to make the notation explicit, while Eqs. (3) – (4) follow established wind-aware UAV routing and multirotor power-modelling literature. Our contribution is the integration, parameter calibration, and the reproducible feasibility-envelope analysis.

For any ordered pair (i, j) define horizontal distance and altitude change (standard coordinate geometry and height-difference convention) [22], [23]:

$$d_{ij} = \sqrt{(x_i - x_j)^2 + (y_i - y_j)^2},$$
$$\Delta h_{ij} = h_j - h_i. \quad (1)$$

Eq. (1) gives the standard Euclidean distance when coordinates are projected (e.g., UTM). In the case study, all horizontal distances are computed with the haversine metric (Section 4.1)

3.2 Travel time under wind

Let $\mathbf{w}_{ij}$ denote the local horizontal wind vector along segment, (i, j) and $\mathbf{u}_{ij}$ the unit vector of the planned ground-track. We define $w_{ij} \geq 0$ as the along-track headwind component (positive for headwind), so that headwind reduces ground speed. Here $\mathbf{w}$ denotes the air-mass velocity vector (direction 'toward'); therefore $w_{\parallel} > 0$ corresponds to headwind along $\hat{\mathbf{u}}$. The along-track wind component is defined via the scalar projection (dot product) [24]:

$$w_{ij}^{\parallel} = -\,\mathbf{w}_{ij} \cdot \mathbf{u}_{ij}. \quad (2)$$

Given commanded airspeed $v_a > 0$, we model segment time using standard wind-triangle kinematics and wind-aware routing formulations [18], [25]:

$$t_{ij} = \frac{d_{ij}}{v_a - w_{ij}^{\parallel}}, v_a - w_{ij}^{\parallel} > \epsilon. \quad (3)$$

Assumption (track-aligned wind): In the reported envelopes we consider a headwind-only setting, i.e., wind is assumed aligned with the planned ground-track and crosswind is negligible $(w_{ij}^{\perp} \approx 0)$. Under this assumption Eq. (3) is valid with $v_a$interpreted as the effective airspeed component aligned with the planned track. For non-negligible crosswind, maintaining the planned track additionally requires $| w_{ij}^{\perp} | < v_a$.

This choice is consistent with the load wind coupling highlighted in the routing literature, where flight time is dependent on the weight of packages in a windy environment.

3.3 Mass and energy feasibility

Let m_{ij} be the vehicle mass on segment (i, j) (airframe + battery + remaining payload). We adopt a compact, calibratable power model suitable for planning and sensitivity analysis. Following closed-form multirotor power modelling approaches [26] (and consistent with multirotor energy modelling used in drone routing [11]), we use the parametric form: $m_{ij}(i, j)$

$$P_{ij} = a\, m_{ij}^{3/2} + b\, v_a^3 + c, \quad (4)$$

This reduced-form parametrization is literature-inspired. Our contribution is the

calibration of coefficients for the reference platform/scenario and its integration into the reproducible feasibility-envelope analysis. Coefficients are identified from manufacturer specifications or flight measurements: a, b, c

In the case study (Section 4), we use the reduced form specialization $(m) = k\, m^{3/2}$, i.e., (4) with $b = 0$, $c = 0$, and $a \equiv k$, to keep the feasibility envelope transparent and straightforward to reproduce.

Air-density effects with altitude can be incorporated through a standard atmosphere mapping $\rho(h)$by treating the power-model coefficients as density-dependent (e.g., $a = a(\rho)$, $b = b(\rho)$). In this demonstrator the coefficients are calibrated at a representative density for the study area.

Segment energy is (standard energy–power relation, E =P·t [27])

$$E_{ij} = P_{ij}\, t_{ij}. \qquad (5)$$

For a route π, total mission energy is (additive path-cost aggregation; see e.g., [28]):

$$E(\pi) = \sum_{(i,j)\in\pi} E_{ij} + \sum_{i\in\pi} E_i^{\mathrm{svc}}, \qquad (6)$$

where E_i^{svc} accounts for service/hover energy at node i(drop-off or handling). The mission is feasible under an available battery energy E_{avail} and reserve policy α (safety margin / SOC threshold practice [29]) if:

$$E(\pi) \le (1-\alpha)\, E_{\mathrm{avail}}. \qquad (7)$$

Here α is an operator-chosen reserve margin. In Section 4 we set α = 0.20 for replicability of the reported envelopes. A conservative treatment of $E_{\mathrm{avail}}$is justified because failing to account for battery performance leads to considerable inaccuracy in estimating the amount of available energy [10].E_{avail}.

3.4 Routing decision variables

Routing is encoded by binary variables $x_{ij} \in \{0,1\}$, where $x_{ij} = 1$ if the UAV flies directly from node i to node j. The optimization objective is defined either as minimizing energy $\sum E_{ij}x_{ij}$ (endurance-limited resupply) or minimizing time $\sum t_{ij}x_{ij}$ (time-critical deliveries), subject to standard routing constraints and feasibility condition (7).

4. CASE STUDY AND QUANTITATIVE EVALUATION

4.1 Operational context and study area (Bucegi Mountains, Romania)

Mountain resupply missions are routinely challenged by terrain accessibility and weather exposure. Logistics drones are particularly attractive for remote locations where access by conventional means is difficult or impossible [7]. At the same time, operational reliability is constrained by weather, since drones cannot fly in all-weather [30].

To keep the practical component reproducible, we define a compact case-study network on the Bucegi plateau and adjacent valley using publicly available coordinates/elevations:

- Sinaia (depot), 45.35000°N 25.55139°E [31] $h = 767$m.
- Cabana Piatra Arsă (plateau micro-hub), 45.383811°N 25.487745°E [32] $h = 1950$m.
- Cabana Babele (customer node), 45.40617°N 25.47201°E [33] m.
- Vârful Omu (high-altitude customer node), 45.4458194°N 25.4563111°E [34].

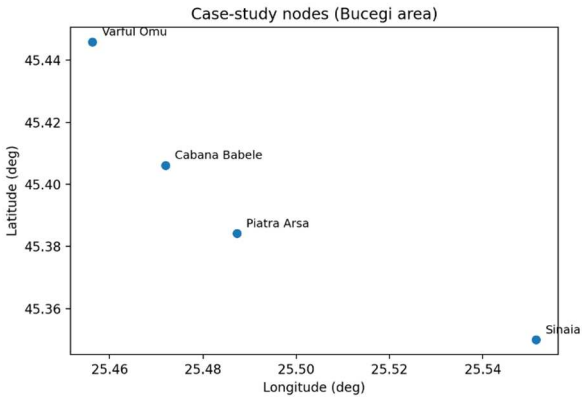


Fig. 1. Case-study nodes in the Bucegi area

All horizontal distances used in the numerical evaluation are computed with the haversine metric (Earth radius 6371 km), ensuring replication of the reported values used in the figures.

4.2 Reference UAV platform and energy budget

We instantiate the demonstration model with a commercially available multirotor [35]. The platform mass used in the computation follows the published specification with two TB65 batteries: Approx. 6.47 kg [35]. Battery energy is taken directly from the TB65 specification Energy: 263.2 Wh so the nominal onboard energy is E batt = 2 × 263.2 = 526.4 Wh [36].

$$E_{\text{batt}} = 2 \cdot 263.2 \text{ Wh} = 526.4 \text{ Wh}.$$

The endurance anchor for calibration is the published value 55 minutes measured while flying at approximately 8 m/s without payloads in a windless environment [35]. We derive an average cruise power anchor $P_0 = E_{\text{batt}}/T_{\text{end}}$. With take off mass m_0(no payload), the coefficient in $P(m) = km^{3/2}$is $k = P_0/m_0^{3/2}$. For $E_{\text{batt}} = 526.4$Wh, $T_{\text{end}} = 55$min, and $m_0 = 6.47$kg, this yields $P_0 \approx 574$W and $k \approx 34.9\text{W} \cdot kg^{-3/2}$.

4.3 Practical mission model and feasibility criterion (replicable)

The evaluation uses an auditable model intended for formula-based verification and graph-based interpretation.

Cruise power calibration (demonstrator). We use a reduced-form multirotor power model

$$P(m) = k\, m^{3/2},$$

where m is take off mass (airframe + batteries + payload). The coefficient k is calibrated from the manufacturer endurance anchor (Section 4.2). More detailed multirotor power modelling approaches are available, including treatments emphasizing closed-form power consumption models [26]. In this case study the cruise airspeed is held fixed ($v_a = 8$ m/s in all reported envelopes), hence any speed-dependent contribution in Eq. (4) is constant at the chosen operating point and can be absorbed into the calibrated coefficient/offset. Consequently, in the reported envelopes wind affects energy primarily through segment time (Eq. 3), rather than through an explicit speed–power coupling; the $P(m)$specialization is not intended for speed optimization.

Wind-aware segment time. We restrict the tested headwind grid to $w \in [0,6]$m/s; with $v_a =$ 8m/s this implies $v_g = v_a - w \geq 2$m/s over all reported results.

Mission energy (out-and-back). To obtain a conservative (worst-case) feasibility envelope, we approximate the out-and-back mission as two identical legs with the same effective headwind $w$and use the takeoff mass $m$for both legs.

$$E_{\text{mission}}(m, w) = 2\, P(m)\, t_{ij} + P(m)\, \tau, + \frac{mg \max(0, \Delta h_{ij})}{\eta_c}$$

where $\Delta h_{ij} = h_j - h_i$and η_c is a climb efficiency factor.

Feasibility criterion (reserve policy). We enforce a fixed energy reserve $\alpha = 0.20$, such that a mission is feasible if:

$$E_{\text{mission}} \leq (1 - \alpha)\, E_{\text{batt}}.$$

All results in Fig. 2, Fig. 3, and Table 1 are computed under exactly this criterion and the parameter set stated above.

4.4 Results: feasibility envelopes and sensitivity analysis

Fig. 2 shows the feasibility envelope for the three out-and-back missions represented in the study: (1) Sinaia ↔ Cabana Babele, (2) Piatra Arsă ↔ Cabana Babele, and (3) Piatra Arsă ↔ Vârful Omu.

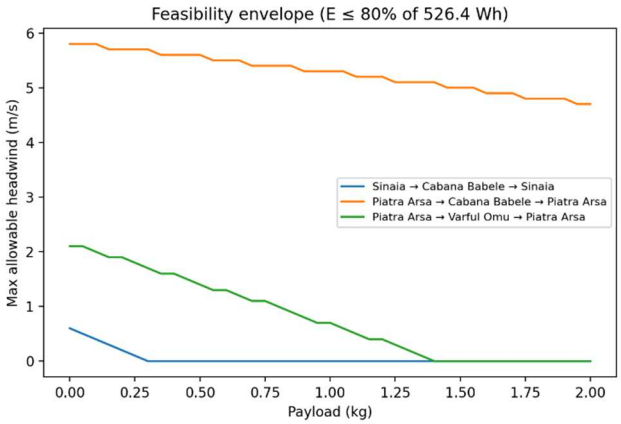


Fig. 2. Feasibility envelope: maximum allowable headwind versus payload for three out-and-back missions

Table 1 reports discrete checkpoint values of w max (allowable headwind within the tested grid) for the same three missions shown in Fig. 2,

computed under the same feasibility criterion and parameter set.

Table 1

Allowable headwind w max within the tested grid (0-6 m/s, step 0.1), by payload level, computed with the same feasibility criterion used in Fig. 2 (E mission ≤ (1–α) E batt, α = 0.20; v a = 8 m/s; service time = 60 s).

Payload (kg)	Sinaia ↔ Cabana Babele: w max (m/s)	Piatra Arsă ↔ Cabana Babele: w max (m/s)	Piatra Arsă ↔ Vârful Omu: w max (m/s)
0.0	0.6	5.8	2.1
0.5	0.0	5.6	1.4
1.0	0.0	5.3	0.7
1.5	0.0	5.0	0.0
2.0	0.0	4.7	0.0

Note. The three routes listed correspond exactly to the three curves in Fig. 2; Fig. 3 provides an energy-vs-payload sensitivity plot for the Piatra Arsă ↔ Vârful Omu mission.

Baseline parameters: a minimal one-at-a-time sensitivity check in $k(\pm 10\%)$, $\alpha(0.15–0.25)$ and $V_a(7–9$ m/s) is summarized below.

Values are conservative, based on the symmetric out-and-back approximation (same headwind and take-off mass on both legs).

Minimal one-at-a-time sensitivity. Using the same feasibility criterion as Table 1, we recomputed the allowable headwind threshold $w_{\max}$while varying:

(i) the calibrated power coefficient $k$by ±10% about k_0;

(ii) the reserve factor αwithin 0.15–0.25;

(iii) the commanded airspeed $V_a$within 7–9 m/s (keeping the same minimum ground-speed constraint $V_a - w \geq 2$m/s).

Across all Table-1 entries, the resulting shift in $w_{\max}$is bounded by $\Delta w_{\max} \leq 0.7$m/s for k, $\Delta w_{\max} \leq 0.6$m/s for α, and $\Delta w_{\max} \leq 1.0$m/s for V_a.

Two patterns are observed. First, valley-to-plateau servicing is wind-sensitive at moderate payloads. Direct Sinaia↔Babele feasibility contracts rapidly with payload under headwind (Fig. 2) [30]. Second, a plateau micro-hub increases the energy margin for high-altitude deliveries. Using Cabana Piatra Arsă as a staging point is practical in operational terms because in summer, it is accessible by car via the paved road from Sinaia. The plateau-origin missions in Fig. 2 preserve a larger feasible region (higher $w_{\max}$ at the same payload), highlighting a benefit at the system level of micro-hub placement in mountain logistics architectures.

Fig. 3 isolates the sensitivity for Piatra Arsă ↔ Vârful Omu: mission energy increases nonlinearly with both payload and headwind due to the combined effects of $m^{3/2}$and $1/(v_a - w)$, producing a sharp feasibility boundary near the headwind limit. This provides a quantitative basis for operational policies such as weather-aware dispatch, payload tiering, and hub-based routing.

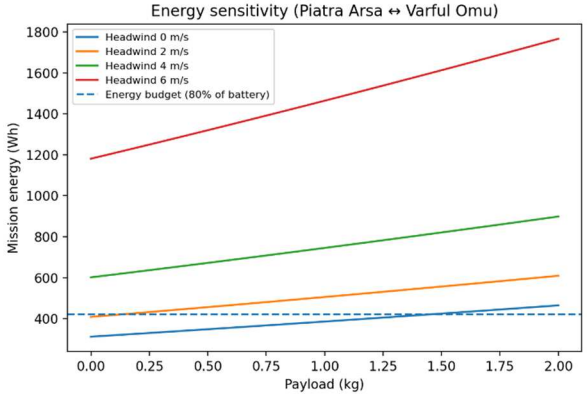


Fig. 3. Mission energy versus payload at selected headwinds for the Piatra Arsă ↔ Vârful Omu out-and-back mission

5. DISCUSSION AND LIMITATIONS

The results (Fig. 2-3, Table 1) show that mountainous resupply feasibility is governed less by geometric distance and more by coupled wind time and load energy effects. In practice, this supports a system architecture in which a plateau micro-hub can expand feasible delivery conditions relative to direct valley-to-plateau sorties, consistent with the operational motivation for using drones in areas where access by conventional means is difficult or impossible [7].

5.1 Operational implications

Envelope-based dispatch can serve as a planning-level decision aid under the stated assumptions. First, for each corridor, a payload-

dependent headwind threshold $w_{\max}(q)$ can be precomputed and used as a clear go/no-go rule (Table 1). Second, the micro-hub strategy reduces exposure to headwinds and climb energy by shortening the heavy-lift segment. This offers a practical in operational terms mechanism for mountainous logistics when a seasonal access window exists to stock the hub.

5.2 Why wind and battery realism matter

The steep energy growth as $w \to v_a$ (Fig. 3) is consistent with the routing observation that flight time is dependent on the weight of packages in a windy environment [18]. Consequently, planning based only on distance is not reliable in mountain corridors. Battery realism is equally critical, since failing to account for battery performance leads to considerable inaccuracy in estimating the amount of available energy [10].

5.3 Limitations and direct extensions

This study uses a compact, reproducible applied model, which implies three limitations.

(i) Wind is represented as a constant along track headwind; crosswinds, gusts, and terrain-driven channelling are not modelled. Accordingly, Eq. (3) is applied under a track-aligned (headwind-only) assumption in the reported feasibility envelopes.

(ii) Power is calibrated via a reduced-form relation rather than a fully decomposed rotorcraft model, although more complete approaches exist where closed form power consumption model in three flight statuses are derived [26]. To partially bound this calibration/operational uncertainty, we report the minimal one-at-a-time sensitivity bounds on $w_{\max}$($\pm 10\%$ in k, $\alpha \in [0.15,0.25]$, $V_a \in [7,9]$m/s) directly after Table 1.

(iii) Vertical motion is simplified to a net ascent term and a fixed service time, omitting path-dependent climb profiles and wind-dependent hover losses. These extensions can be implemented without changing the planning logic. Replace the wind scalar with corridor specific wind layers (and robust bounds), substitute a richer closed form power model, and compute energy on segmented vertical profiles. The out-and-back energy model is intentionally conservative (symmetric headwind and take off mass on both legs) to support go/no-go dispatch rules. A refined variant could account for tailwind on return and reduced mass after delivery, which would expand the feasible region.

6. CONCLUSIONS

We propose and evaluate a reproducible feasibility screening test for mountainous UAV resupply that couples wind-dependent segment time, payload-dependent power, and an explicit battery-reserve policy, reported as feasible payload–headwind envelopes and sensitivity curves linking engineering-level modelling to planning-level dispatch screening.

The operational statements below are limited to the planning model used here (track-aligned steady headwind, reduced-form cruise power calibrated at a single operating point, symmetric out-and-back approximation, and nominal battery energy with a fixed reserve). Accordingly, the reported envelopes should be interpreted as conservative screening results for this case study and parameterization, not as full operational validation.

Key conclusions from the model-based (numerical) evaluation are:

A sharp wind threshold emerges at fixed commanded airspeed. As along-track headwind approaches the commanded airspeed, mission time increases rapidly and energy demand rises steeply, creating an operational cliff where small wind changes can switch a sortie from feasible to infeasible.

A plateau micro-hub enlarges the feasible delivery region for high-altitude nodes. Compared with direct valley-to-plateau servicing, staging from a plateau-accessible hub reduces the combined distance–climb burden per sortie, enabling higher feasible headwinds at the same payload under the stated assumptions and supporting a resilient last-mile architecture.

The model yields conservative dispatch screening maps under stated assumptions. The derived relationship between payload tier and

maximum allowable headwind provides a clear go/no-go screening map under a fixed reserve policy across the tested headwind range; operational use should be complemented by platform flight validation and local wind/battery condition assessments.

Future work should increase operational fidelity through flight-test validation and by relaxing key assumptions (non-steady winds, additional wind components, richer power modelling, and battery state variability).

7. REFERENCES

[1] Options Consultancy Services, *Flying medicines over mountains: Nepal drones last mile delivery innovation,* Options Consultancy Services, 2021. [Online]. Available: https://options.co.uk/wp-content/uploads/2021/04/Flying-medicines-over-mountains-Nepal-drones-last-mile-delivery-innovation.pdf

[2] P. Thapa and M. Thapa, *Operational efficiency and environmental impact of UAV-based vaccine delivery in remote areas of Nepal,* Res., vol. 2, no. 2, p. 100207, Jun. 2025, doi: 10.1016/j.nexres.2025.100207.

[3] J. Chute, *UNICEF Guidance on the Use of Drones in Supply Chains,* UNICEF Supply Division, 2021. [Online]. Available: https://www.unicef.org/supply/media/10326/file/UNICEF-Guidance-on-use-of-drones-in-supply-chains.pdf

[4] A. M. Knoblauch et al., *Bi-directional drones to strengthen healthcare provision: experiences and lessons from Madagascar, Malawi and Senegal,* BMJ Glob. Health, vol. 4, no. 4, p. e001541, Jul. 2019, doi: 10.1136/bmjgh-2019-001541.

[5] IDinsight, *Zipline Brief (Digital v3),* IDinsight, 2022. [Online]. Available: https://www.idinsight.org/wp-content/uploads/2022/06/Zipline-Brief-FINAL-Digital-v3.pdf

[6] M. P. Nisingizwe et al., *Effect of unmanned aerial vehicle (drone) delivery on blood product delivery time and wastage in Rwanda: a retrospective, cross-sectional study and time series analysis,* Lancet Glob. Health, vol. 10, no. 4, pp. e564–e569, Apr. 2022, doi: 10.1016/S2214-109X(22)00048-1.

[7] G. Minculete, *Military Logistics Drones: The Innovative Solution for Transportation Challenges on the Battlefield,* Land Forces Acad. Rev., vol. 30, no. 2(118), pp. 342–354, 2025, doi: 10.2478/raft-2025-0033.

[8] European Commission, *Commission Implementing Regulation (EU) 2021/664 of 22 April 2021 on a regulatory framework for the U-space (Text with EEA relevance).* Apr. 2021. [Online]. Available: https://eur-lex.europa.eu/eli/reg_impl/2021/664/oj/eng

[9] International Civil Aviation Organization, *Unmanned Aircraft Systems Traffic Management (UTM) – A Common Framework with Core Principles for Global Harmonization,* International Civil Aviation Organization, 2023. [Online]. Available: https://www.icao.int/sites/default/files/left-menu-pdfs/UTM%20Framework%20Edition%204.pdf

[10] M. Beigi, M. Rajabi, and M. Aghakhani, *An Overview of Drone Energy Consumption Factors and Models.* 2022. doi: 10.48550/arXiv.2206.10775.

[11] K. Dorling, J. Heinrichs, G. G. Messier, and P. Magierowski, *Vehicle Routing Problems for Drone Delivery,* IEEE Trans. Syst. Man Cybern. Syst., vol. 47, no. 1, pp. 70–85, 2017, doi: 10.1109/TSMC.2016.2582745.

[12] R. Liu, H. Shin, M. Seo, and A. Tsourdos, *Energy-aware Route Planning for Drone Delivery Systems,* in CEAS EuroGNC 2022 – Conference on Guidance, Navigation and Control, Berlin, Germany, May 2022. [Online]. Available: https://eurognc.ceas.org/archive/EuroGNC2022/pdf/CEAS-GNC-2022-045.pdf

[13] W. Liu, W. Li, Q. Zhou, Q. Die, and Y. Yang, *The Optimization of the 'UAV-Vehicle' Joint Delivery Route Considering Mountainous Cities,* PLOS ONE, vol. 17, no. 3, p. e0265518, Mar. 2022, doi: 10.1371/journal.pone.0265518.

[14] M. Østbø, P. Osen, G. Rokseth, O. V. Homleid, and T. Sevaldrud, *Exploiting Meteorology to Enhance the Efficiency and Safety of UAV Operations,* Norwegian Defence Research Establishment (FFI), FFI/RAPPORT-2004/00981, Mar. 2004. [Online]. Available: https://www.ffi.no/publikasjoner/arkiv/exploiting-meteorology-to-enhance-the-efficiency-and-safety-of-uav-operations

[15] A. Oakey, T. Cherrett, J. Green, and J. Dickinson, *Quantifying Weather Tolerance Criteria for Delivery Drones – A UK Case Study,* in 2023 International Conference on Unmanned Aircraft Systems (ICUAS), Warsaw, Poland, Jun. 2023, pp. 1005–1012. doi: 10.1109/ICUAS57906.2023.10156144.

[16] L. Palazzetti, C. M. Pinotti, and G. Rigoni, *A Run in the Wind: Favorable Winds Make the Difference in Drone Delivery,* in 2021 17th International Conference on Distributed Computing in Sensor Systems (DCOSS), Jul. 2021, pp. 109–116. doi: 10.1109/DCOSS52077.2021.00031.

[17] F. Yacef, N. Rizoug, O. Bouhali, and M. Hamerlain, *Optimization of Energy Consumption for Quadrotor UAV,* in Proceedings of the 9th International Micro Air Vehicle Conference and Competition (IMAV 2017), 2017. [Online]. Available: https://www.imavs.org/papers/2017/31.pdf

[18] S. Ito et al., *Load and Wind Aware Routing of Delivery Drones,* Drones, vol. 6, no. 2, p. 50, 2022, doi: 10.3390/drones6020050.

[19] F. Betti Sorbelli, F. Corò, S. K. Das, and C. M. Pinotti, *Energy-Constrained Delivery of Goods with Drones Under Varying Wind Conditions.* 2020. doi: 10.48550/arXiv.2012.08602.

[20] C. Cheng, Y. Adulyasak, L.-M. Rousseau, and M. Sim, *Robust Drone Delivery with Weather Information,* 2020, [Online]. Available: https://hanalog.ca/wp-content/uploads/2020/07/7897.pdf

[21] ESSP and EUSPA, *EGNOS Guidelines for Low-Risk UAS Operations,* European Satellite Services Provider (ESSP) and European Union Agency for the Space Programme (EUSPA), Version 01-00, Mar. 2025. [Online]. Available: https://egnos.gsc-europa.eu/sites/default/files/2025-03/Guidelines%20for%20EGNOS%20in%20low-risk%20UAS%20operations.pdf

[22] P. Brown, M. Evans, D. Hunt, J. McIntosh, B. Pender, and J. Ramagge, *Introduction to Coordinate Geometry: A guide for teachers – Years 9–10* (TIMES Project, Module 29).

Australian Mathematical Sciences Institute (AMSI) / ICE-EM, The University of Melbourne, 2011. [Online]. Available: https://amsi.org.au/teacher_modules/pdfs/Introduction_to_coordinate_geometry.pdf

[23] K. Dawidowicz, *Analysis of Height Determination Using the ASG-EUPOS NAWGEO Service,* Tech. Sci., vol. 16, no. 1, pp. 19–39, 2013, [Online]. Available: https://yadda.icm.edu.pl/baztech/element/bwmeta1.element.baztech-97e16ee3-a626-433d-be22-d5903ca18533/c/Dawidowicz.pdf

[24] O. Shatalov, *Section 1.2: The Dot Product.* 2012. [Online]. Available: https://people.tamu.edu/~shatalov68/151LN_section1.2.pdf

[25] R. W. Beard and T. W. McLain, *Guidance and Control of Autonomous Miniature Air Vehicles.* 2010. [Online]. Available: https://www.et.byu.edu/~beard/classes/ece674/uavbook.pdf

[26] H. Gong, B. Huang, B. Jia, and H. Dai, *"Modelling Power Consumptions for Multi-rotor UAVs."* Sep. 2022. doi: 10.48550/arXiv.2209.04128.

[27] Physics LibreTexts, *Power.* [Online]. Available: https://phys.libretexts.org/Bookshelves/University_Physics/Physics_(Boundless)/06%3A_Uniform_Circular_Motion_and_Gravitation/6.06%3A_Power

[28] P. Munari, T. Dollevoet, and R. Spliet, *A generalized formulation for vehicle routing problems,* Sep. 2017, [Online]. Available: https://arxiv.org/pdf/1606.01935

[29] C. Kulkarni, E. Hogge, and C. C. Quach, *Remaining Flying Time Prediction Implementing Battery Prognostics Framework for Electric UAV's,* in AIAA Propulsion and Energy Forum, Cincinnati, OH, USA, Jul. 2018. [Online]. Available: https://ntrs.nasa.gov/citations/20180004466

[30] M. Gao, C. H. Hugenholtz, T. A. Fox, M. Kucharczyk, T. E. Barchyn, and P. R. Nesbit, *Weather Constraints on Global Drone Flyability,* Sci. Rep., vol. 11, no. 1, p. 12092, 2021, doi: 10.1038/s41598-021-91325-w.

[31] Google Maps, *Coordinate point: 45°21'00.0"N 25°33'05.0"E (45.35, 25.55139).* 2026. [Online]. Available: https://www.google.com/maps/place/45%C2%B021'00.0%22N+25%C2%B033'05.0%22E/@45.35,25.5488151,17z/data=!3m1!4b1!4m4!3m3!8m2!3d45.35!4d25.55139?entry=ttu&g_ep=EgoyMDI2MDExMy4wIKXMDSoASAFQAw%3D%3D

[32] Google Maps, *Coordinate point: 45°23'01.7"N 25°29'15.9"E (45.383811, 25.487745).* 2026. [Online]. Available: https://www.google.com/maps/place/45%C2%B023'01.7%22N+25%C2%B029'15.9%22E/@45.383811,25.4851701,17z/data=!3m1!4b1!4m4!3m3!8m2!3d45.383811!4d25.487745?entry=ttu&g_ep=EgoyMDI2MDExMy4wIKXMDSoASAFQAw%3D%3D

[33] Google Maps, *Coordinate point: 45°24'22.2"N 25°28'19.2"E (45.40617, 25.47201).* 2026. [Online]. Available: https://www.google.com/maps/place/45%C2%B024'22.2%22N+25%C2%B028'19.2%22E/@45.40617,25.4694351,17z/data=!3m1!4b1!4m4!3m3!8m2!3d45.40617!4d25.47201?entry=ttu&g_ep=EgoyMDI2MDExMy4wIKXMDSoASAFQAw%3D%3D

[34] Google Maps, *Coordinate point: 45°26'45.0"N 25°27'22.7"E (45.4458194, 25.4563111).* 2026. [Online]. Available: https://www.google.com/maps/place/45%C2%B026'45.0%22N+25%C2%B027'22.7%22E/@45.4458194,25.4537362,17z/data=!3m1!4b1!4m4!3m3!8m2!3d45.4458194!4d25.4563111?entry=ttu&g_ep=EgoyMDI2MDExMy4wIKXMDSoASAFQAw%3D%3D

[35] DJI, *Matrice 350 RTK – Specs.*Available: https://enterprise.dji.com/matrice-350-rtk/specs

[36] DJI, *TB65 Intelligent Flight Battery – Specs.* Available: https://enterprise.dji.com/tb65/specs

Modelarea fezabilității, sensibilă la vânt și încărcătură, pentru reaprovizionarea în munți cu UAV: studiu de caz reproductibil în Munții Bucegi

Rezumat: Prezentăm un cadru de lucru reproductibil, formulat pe baza unor ecuații, pentru reaprovizionarea cu UAV în teren montan, în care fezabilitatea este determinată de efectele interdependente vânt frontal timp și sarcină utilă energie. Un model simplificat de putere pentru multirotor, o estimare a timpilor pe segmente care ține cont de vânt și o politică explicită de rezervă a bateriei sunt integrate într-un singur test de fezabilitate, vizualizat prin diagrame vânt frontal sarcină utilă și curbe de sensibilitate energetică. Metoda este demonstrată pe o rețea din Munții Bucegi (depozitul Sinaia, micro-hub-ul Piatra Arsă, Babele și Omu) și permite formularea unor reguli operaționale de decizie (go/no-go) pe intervale de sarcină utilă, inclusiv un prag pronunțat (wind cliff) atunci când vântul frontal se apropie de limita vitezei aeriene impuse (testat până la 6 m/s).

Gheorghe MINCULETE, Professor, PhD, "Nicolae Bălcescu" Land Forces Academy of Sibiu, Department of Economic Sciences, minculetegh@yahoo.com, +40 269 432 990, 3-5 Revolutiei Street, Sibiu, Romania.

Dragoș GHERGHINOIU, PhD Student, "Nicolae Bălcescu" Land Forces Academy of Sibiu, Military training centre, dragosgherghinoiu@gmail.com, +40 269 432 990, 3-5 Revolutiei Street, Sibiu, Romania.